Optically Stimulated Luminescence Dating of Sediments over the Past 200,000 Years

Edward J. Rhodes

Department of Earth and Space Sciences, University of California, Los Angeles,
California 90095-1567; email: erhodes@ess.ucla.edu

Keywords

optical dating, sediment, Quaternary, paleoenvironment, geochronology,
OSL

Abstract

Optical dating of sediment using optically stimulated luminescence has be-
come important for studying Earth surface processes, and this technique
continues to develop rapidly. A group of closely linked luminescence meth-
ods can be used to estimate the time since grains of quartz and feldspar
were last exposed to daylight by detecting their subsequent response to en-
vironmental ionizing radiation exposure. The technique is well suited to the
dating of deposits as young as one year to several hundred thousand years.
Recent technical developments have established a dating protocol with im-
proved precision, a high degree of reliability, and an in-built means to detect
incomplete signal removal during deposition. This approach has been ex-
tended to age estimation for single grains, opening up a wider range of
potential environments and new possibilities for understanding postdepo-
sitional grain movement. Ongoing research offers the possibility of signifi-
cant age range extension and novel applications including low-temperature
thermochronology.

1. INTRODUCTION

OSL: optically stimulated luminescence

Dose rate: the radiation dose absorbed each year (measured in Gy·year^{-1})

Gy: Gray, SI unit of radiation dose (1 Gy = 1 J·kg^{-1})

Sensitivity: the luminescence generated (OSL signal size) in response to one unit of dose

TL: thermoluminescence

IRSL: infrared stimulated luminescence

Stimulation: incident light that causes detrapping of charge

SAR: single aliquot regenerative-dose

Optical dating of sediments using optically stimulated luminescence (OSL) signals in mineral grains began in 1985 (Huntley et al. 1985). This exciting new technique dates deposition back to 200,000 years or more and has experienced recent rapid expansion in use. Applications cover many areas of Earth and environmental sciences, and it is widely used in archaeological and anthropologic contexts (Aitken 1998). In essence, the method is similar to radiation damage techniques (e.g., fission track dating) and comprises four steps: (*a*) removal of trapped charge within mineral grains by natural daylight exposure during transport, (*b*) gradual buildup of charge as buried grains are exposed to environmental radiation, (*c*) sample collection and OSL measurement of trapped charge concentration, and (*d*) determination of the environmental dose rate experienced by grains at each sample location.

The technique has huge potential for understanding Earth and planetary surface processes. OSL has extraordinary sensitivity to environmental conditions, namely signal erasure in seconds by daylight or by heating in the range of 200°C to 400°C. Furthermore, the minerals most commonly used in OSL, quartz and feldspar, are virtually ubiquitous in terrestrial surface settings. Providing an age range from one year to several hundred thousand, and with indications that the upper limit will soon be extended by an order of magnitude, the method helps fill the gap between observational process studies and events dated by radiometric methods that depend on crystallization. The technique complements other Quaternary dating methods, including radiocarbon (^{14}C), uranium series methods, and cosmogenic nuclide techniques and benefits from an extremely wide range of applicable contexts (**Figure 1**).

Luminescence dating includes the techniques of thermoluminescence (TL) (Aitken 1985), in which mineral grains are heated during measurement, and optical dating (Huntley et al. 1985, Aitken 1998), in which samples are exposed to an intense light source to evict charge from only light-sensitive traps. Optical dating uses the OSL signal of quartz (Smith et al. 1986) or feldspar (Godfrey-Smith et al. 1988) or the infrared stimulated luminescence (IRSL) (Hütt et al. 1988) signals of feldspar. Also, used interchangeably with the name optical dating are the terms photostimulated luminescence and green light stimulated luminescence, besides other names.

With different stimulation wavelengths, a choice of minerals and grain sizes, and several measurement procedures, this related group of techniques can be confusing. However, one measurement protocol stands out, namely the quartz OSL single aliquot regenerative-dose (SAR) protocol of Murray & Wintle (2000, 2003), owing to its apparent accuracy and reliability (Murray & Olley 2002, Rhodes et al. 2003). It provides improved dating precision in comparison with previous luminescence dating methods and incorporates an assessment of internal consistency, allowing problems related to incomplete signal zeroing at deposition to be clearly identified, and in many cases mitigated. Using SAR, OSL age estimates may be determined for single quartz grains (Murray & Roberts 1997), an approach now applied routinely to help overcome limitations provided by incomplete signal zeroing in environments such as caves (e.g., Henshilwood et al. 2002) or flood deposits (e.g., Rhodes et al. 2010).

It is the aim of this review to explain the basis of OSL dating, to identify the most important elements and applications, and to illustrate ways in which these methods can be used. In addition, emerging developments are briefly explored and future directions highlighted. For simplicity and clarity, I have restricted the discussion mostly to OSL and concentrate attention on the quartz SAR protocol.
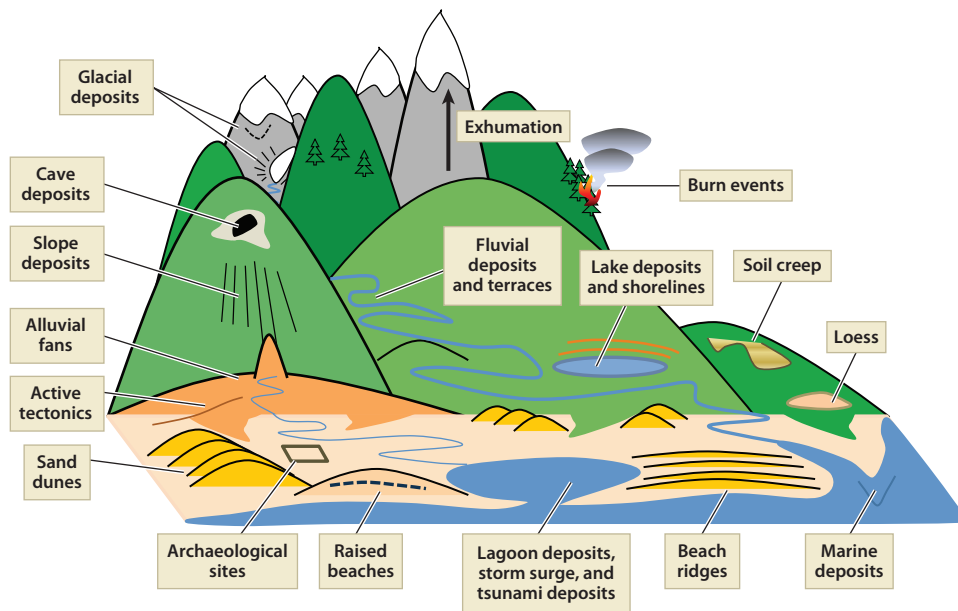
Figure 1

Cartoon illustration of the main environments in which optically stimulated luminescence (OSL) can be applied on timescales of 1 year to ~200,000 years, depending on site and sample characteristics. In particular, the method has contributed significantly to studies of Quaternary glaciation, dune building, fluvial activity, and loess records. The applicability of OSL depends on both environmental factors and sample characteristics. Some applications are well established (e.g., dating dunes or loess), whereas others are under development (e.g., thermochronology, wild fire reconstruction).

2. BASIS OF THE TECHNIQUE

Natural environmental radiation causes charge (electrons and holes) to become trapped when grains are buried in the ground, as bonding electrons are excited from their valence positions, and a small fraction become trapped within the crystal lattice (**Figure 2**). Electron and hole traps are formed at point defects such as those formed by elemental substitution, for example, where Ti replaces Si in quartz. Charge may be compensated by the presence of alkali ions, for example, species such as an electron trap $[TiO_4/Li^+]°$, or the hole center $[AlO_4]°$, known from electron paramagnetic resonance studies (e.g., Weil 1984). Although several models have been proposed (e.g., Itoh et al. 2002), the detailed structure of the OSL electron traps in quartz continues to be explored; the Al hole center mentioned above is likely responsible for the quartz OSL emission in the UV region around 360–380 nm (Martini et al. 2009).

Brief heating at 200°C–400°C, or a short daylight exposure (in the range of 1 to 100 s) is sufficient to reduce certain electron trap populations to a low level, effectively resetting the OSL dating clock. The subsequent gradual increase in trapped charge population in response to the prevailing radiation flux provides the basis for dating. Trapped charge concentration is assessed by laboratory OSL measurements, whereas natural radiation flux, or dose rate, may be determined with a choice of methods.
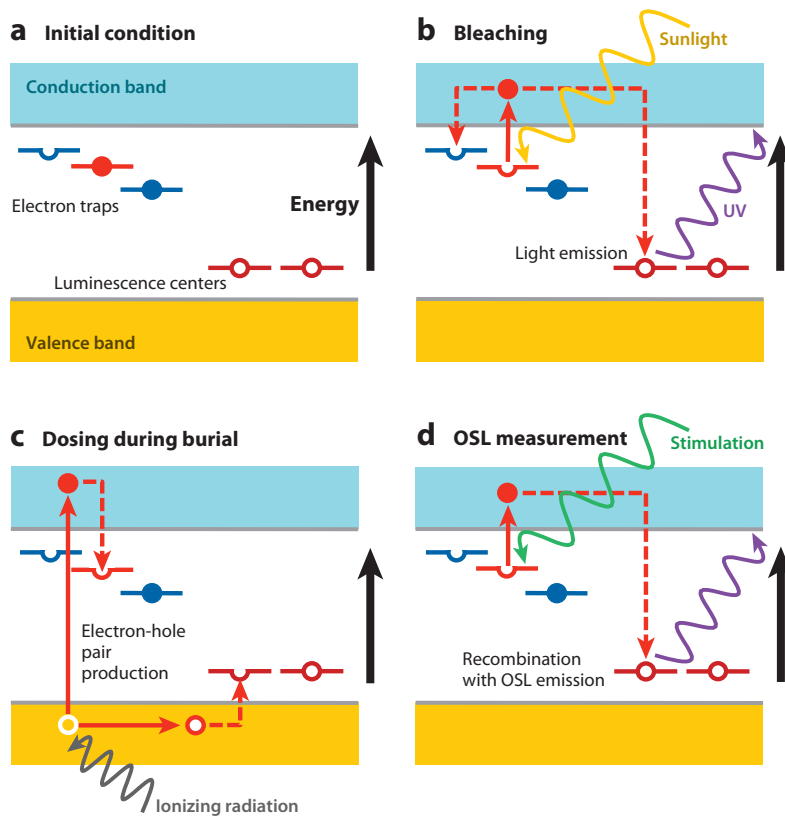
a   Initial condition

b   Bleaching

c   Dosing during burial

d   OSL measurement

Figure 2

Simple band gap energy model of optically stimulated luminescence (OSL). Light-sensitive (OSL) electron traps are shown in red, light-insensitive (thermoluminescence) traps in blue. (*a*) Under typical initial conditions, low thermal stability traps close to the conduction band are kept empty by thermal eviction at ambient temperature, but other traps are filled; luminescence centers are available. (*b*) On light exposure, electrons in OSL traps are evicted and may become trapped in other available trapping sites or may recombine at hole centers (luminescence centers). After brief light exposure, all OSL traps are emptied. (*c*) During subsequent burial, ionizing radiation gradually produces electron-hole pairs, some of which may become trapped, increasing the OSL trap population. (*d*) Following collection and mineral separation, intense blue-green stimulating light is directed at the sample. Electrons are evicted from OSL traps and recombine at luminescence centers, emitting UV luminescence, detected through glass filters with a photomultiplier tube. As the remaining OSL trap populations falls, the emission rapidly decays to a low level.

Recombination of electrons at luminescence centers, similar to those responsible for cathodo-luminescence, provides OSL, IRSL and TL emissions, although the electron source is different for cathodoluminescence. OSL signals consist of a rapidly decaying light emission as electrons are evicted, which, for quartz, represents the sum of several single exponential decay components from discrete trap types (Bailey et al. 1997), whereas in feldspar, a continuum of traps produces a more complex decay form (**Figure 3**).

The storage of trapped charge within the crystal lattice is similar to the action of a rechargeable battery, forming an attractive analogy (Duller 2008). One important distinction is that in luminescence dating, charging occurs very slowly (10^1–10^5 years), but charge removal (battery use) happens very quickly (10^0–10^2 s) during both bleaching and OSL measurement (**Figure 4**).

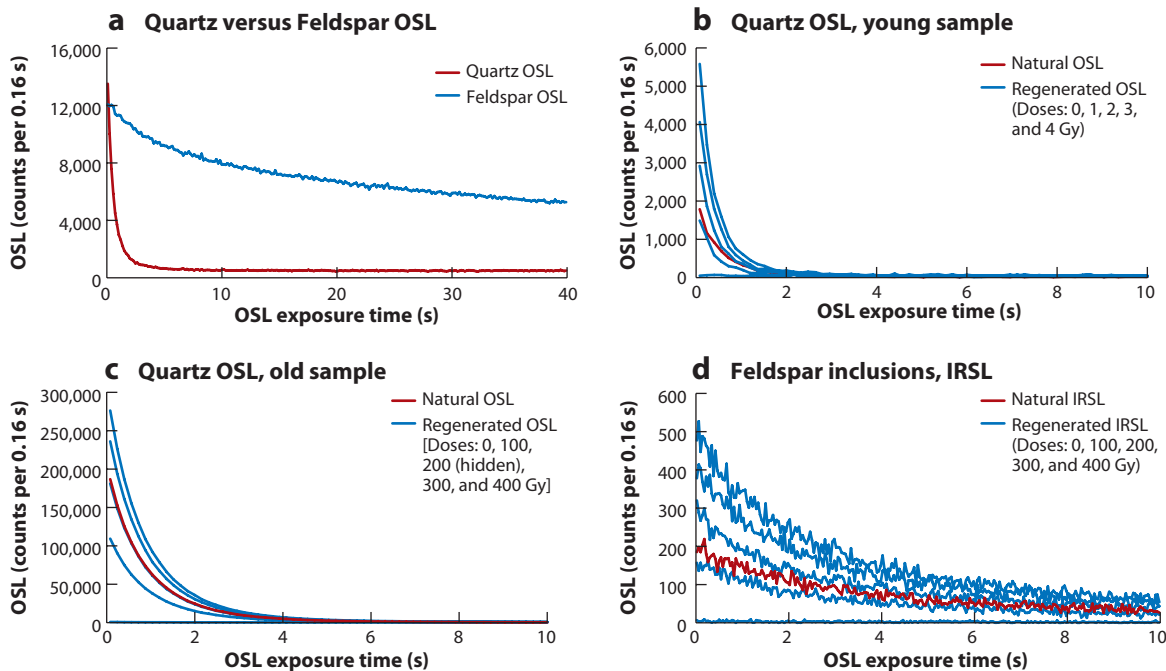**Bleaching:** the removal of trapped charge by light exposure

Figure 3

Examples of optically stimulated luminescence (OSL) and infrared stimulated luminescence (IRSL) decay curves. Luminescence is emitted in the UV when the sample is stimulated by intense light, typically blue-green (470 ± 20 nm) light in the case of OSL and infrared (880 ± 80 nm) for IRSL. All measurements were performed at raised temperature: 125°C for OSL and 60°C for IRSL. (*a*) Note the different shape of quartz and feldspar OSL decays. (*b*) Natural (*red*) and regenerative-dose (*blue*) OSL decays for one aliquot (portion) of a young Australian fluvial quartz sample. The equivalent dose (D_e) is estimated by comparing the initial natural OSL intensity with that regenerated by different laboratory doses. (*c*) Natural (*red*) and regenerative-dose (*blue*) OSL decays for an aliquot of quartz grains from an Australian dune deposited approximately 200,000 years ago, with a D_e value of around 200 Gy [Gy stands for Gray, the SI unit of radiation dose (1 Gy = 1 J·kg^{-1})]. (*d*) IRSL signals from feldspar inclusions contained within quartz grains. Aliquots displaying little sensitivity change were selected.

2.1. Optically Stimulated Luminescence Age Determination

Three principal components required for luminescence age estimation are (*a*) natural luminescence signal measurement, (*b*) an assessment of sensitivity (luminescence signal response to applied radiation dose), and (*c*) determination of the burial dose rate experienced by each sample. The first two components are combined into a single procedure that provides the applied dose acquired over the period of interest. This represents the radiation energy deposited within the crystal since last daylight exposure during transport through the environment (or heating), referred to as the equivalent dose, or D_e, measured in the SI unit Grays (Gy; 1 Gy = 1 J·kg^{-1}). Sample age is calculated by dividing the equivalent dose value by the mean dose rate:

$$age(years) = D_e(Gy)/dose\ rate\ (Gy\ year^{-1}). \qquad (1)$$

Different methods to determine D_e and dose rate are presented below; **Figure 5** presents an overview of the OSL dating process, including key inputs and steps.

The lower age limit lies in the range of months (possibly weeks) to years, restricted only by signal sensitivity and thermal transfer components (signals generated on heating, representing charge

D_e: equivalent dose, the radiation energy absorbed since the OSL signal was set to zero

a Rapid bleaching

Trapped charge reduction by daylight in environment

b Gradual dosing

During burial, trapped charge builds up by ionizing radiation exposure

c OSL measurement

Trapped charge evicted by stimulating light recombines and emits OSL
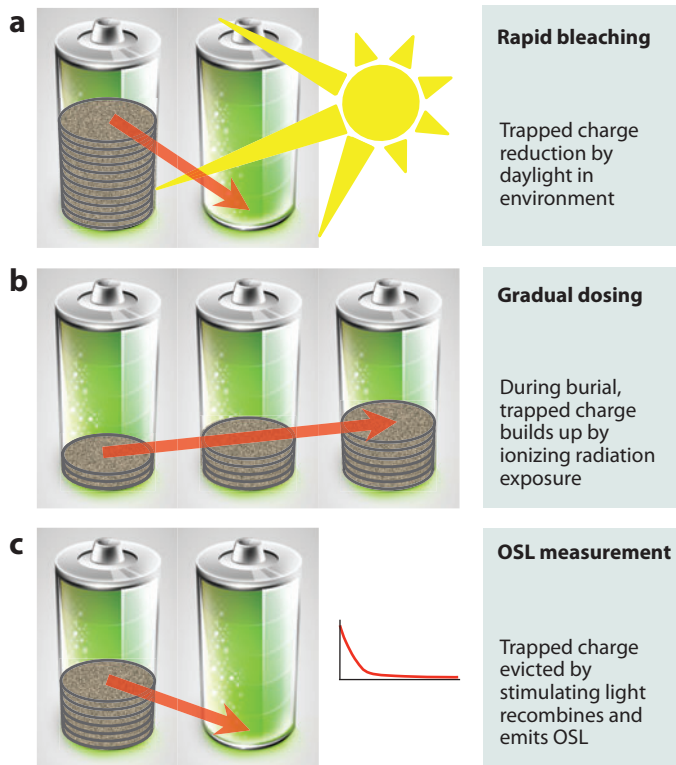
Figure 4

The rechargeable battery forms a useful analogy to help understand optically stimulated luminescence (OSL) dating; gray circles show charge level. (*a*) Daylight releases trapped charge during grain movement over periods of seconds to minutes. (*b*) Charge is slowly built up as a small fraction of electron-hole pairs produced by low levels of environmental radiation are trapped at defects. (*c*) After sample collection and preparation, intense stimulating light releases charge from light-sensitive traps, which recombines emitting UV luminescence, in the form of an OSL decay (shown). Based on an illustration by Duller (2008).

relocation from other trapping centers). The upper age limit is controlled by dose saturation, where all suitable traps have become filled, and extended exposure to radiation results in no further trapping of charge. Age estimates are quoted as a central value with 1σ (68%) uncertainty (typically $\pm$ 5 to 10%), usually in years before present (i.e., publication date).

2.2. Measurement Equipment

OSL (and IRSL) measurement is performed at raised temperature (50°C–160°C), illuminating the sample with intense stimulation light. For OSL, light-emitting diodes (LEDs) with peak emission at 470 nm (blue-green) or green laser emission at 532 or 514 nm are used, whereas for IRSL, LEDs and laser or laser diode sources in the range of 800–900 nm are employed. Signal detection utilizes a photomultiplier tube through a glass filter, designed to pass UV light but exclude OSL and IRSL stimulation wavelengths. Several systems are used, but the Risø automated luminescence reader is widely employed (**Figure 6**) (Bøtter-Jensen et al. 2000). This equipment holds up to 48 1-cm-diameter sample aliquots (portions) and is programmed to give a series of OSL, IRSL, irradiation, and heating treatments to each aliquot.

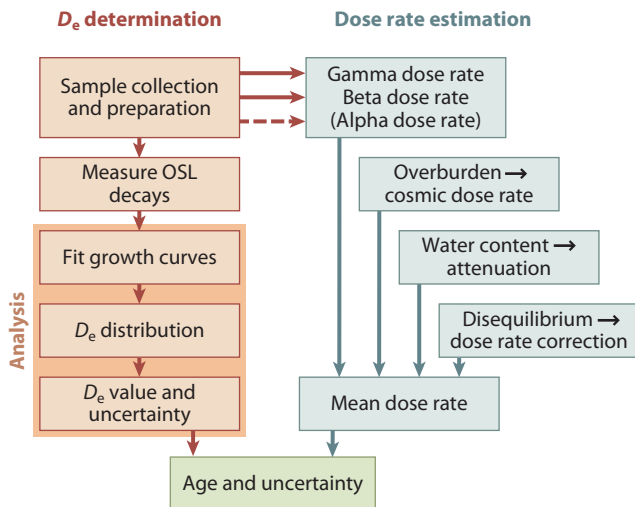**Saturation:** when all OSL traps are full, and no further growth occurs with applied dose

Figure 5

Inputs and key steps in optically stimulated luminescence (OSL) dating. Boxes on the left indicate steps in equivalent dose (D_e) determination, and those on the right represent elements of dose rate estimation.

3. PRACTICAL CONSIDERATIONS

Luminescence characteristics and behavior vary widely even for single composition minerals such as quartz. Consequently, there is no universal best approach for OSL dating; in particular circumstances different approaches may result in the most precise and accurate age estimates with meaningful uncertainty values. The primary aspects that may be varied include

1. Mineral: quartz, K feldspar, or polymineral sample
2. Grain size: sand-sized or silt-sized
3. Measurement method: SAR, multiple aliquot additive dose, or other
4. Dose rate determination method

3.1. Mineral Selection

The quartz fast component (Smith & Rhodes 1994) provides age estimates in good agreement with independent control in a wide range of contexts (Murray & Olley 2002, Rhodes et al. 2003, Rittenour 2008). However, when grains were eroded recently from bedrock, low sensitivity and other issues make this approach difficult, particularly in Arctic (and Antarctic) contexts, in high mountain environments, some glaciated terrains, and tectonically active regions.

K feldspar usually has high OSL (and IRSL) sensitivity with relatively rapid bleaching characteristics. However, many feldspar compositions display an effect termed anomalous fading (Wintle 1973), leading to age underestimation. It is caused by quantum mechanical tunneling; methods have been developed to monitor the fading rate and make suitable corrections (e.g., Huntley & Lamothe 2001, Auclair et al. 2003). Feldspars typically display significantly higher dose saturation levels than quartz, though the decay form (**Figure 3**) is generally more complex. K feldspar also contains an appreciable internal dose rate, adding some complexity to dating.

3.2. Grain Size Selection

In principle, OSL (and IRSL) from any grain size can be measured, but considerations of dose rate estimation, bleaching likelihood, and possibility of postdepositional translocation are important.
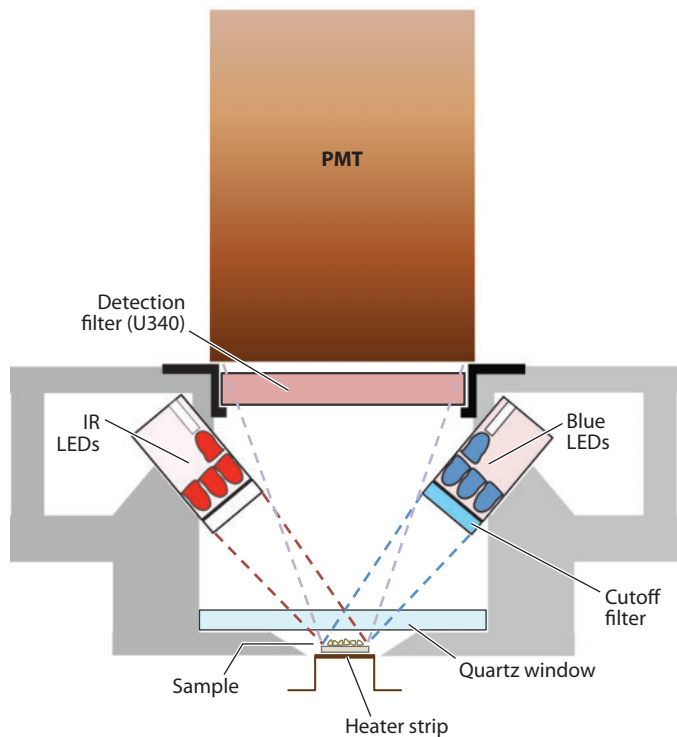
Figure 6

Schematic of a typical optically stimulated luminescence/infrared stimulated luminescence (OSL/IRSL) detection system, based on the Risø TL-DA-20 luminescence reader. The sample (1-cm diameter) is held at raised temperature on a heater plate (which can also be used for thermoluminescence measurement) and illuminated by stimulation wavelengths from blue or IR light-emitting diodes (LEDs). UV luminescence emission is detected through a U340 filter by the photomultiplier tube (PMT).

Two distinct grain-size ranges, referred to as fine-grained (fine silt-sized) and coarse-grained (fine sand and up, e.g., 90–125 μm), are generally used. Fine grains represent those on and below the range of alpha particle track lengths, for which a relatively uniform flux of alpha dosing can be assumed. For coarse-grained samples, the externally alpha irradiated zone of ∼20 μm is removed by etching in hydrofluoric acid, thus eliminating the requirement to consider external alpha dose rates. Grain-size separation for coarse-grained samples uses wet or dry sieving; for fine grains, settling based on Stoke's Law is employed.

4. TRAPPED CHARGE REMOVAL IN NATURE: BLEACHING

Bleaching is the removal by light of the trapped charge populations, sometimes also termed zeroing, although the signal may not be reduced to zero in every case. The rate and completeness of bleaching depends both on environmental factors and sample properties. If a sample contains incompletely zeroed grains, the mean equivalent dose will represent an overestimate, owing to the additional contribution from unwanted residual signals. Improving techniques for the detection of incomplete bleaching and reliable D_e determination represents a significant fraction of ongoing research effort by OSL specialists.

4.1. Environmental Controls on Bleaching

Environmental factors include the intensity and duration of daylight exposure, besides the incident light spectrum. Grains transported within different environments experience diverse amounts of light exposure, ranging from subglacial transport, or in deep karstic systems, where grains may be exposed to no light, to repeated exposure in a tropical beach swash zone. In all environments, grains may be transported at night and receive no light exposure; ~50% of deposition occurs in the dark. An important consideration is the total transport time for each grain and the number of repeated bursts of movement interspersed with temporary halts or shallow burial. The last transport event before deposition is not necessarily the most important, as previous movement can often provide sufficient light exposure for bleaching.

In general, bleaching of light-sensitive traps is quicker with higher energy photons (the UV end of the visible spectrum) and at raised temperatures (thermal assistance), although some traps have bleaching resonances such as K feldspar IRSL source traps (Hütt et al. 1988). Deep water attenuates the UV end of the spectrum (hence the green color of deep water), reducing bleaching rates.

Finer grains are more likely to be transported as suspended load and, therefore, be brought to the surface. However, poorly sorted flood sediments may represent a mixture of unbleached fine grains from bank erosion and well-bleached sand grains from the channel.

4.2. Luminescence Characteristics: Sample Bleachability

Luminescence characteristics are important for sample bleachability, the bleaching rate, and residual signal levels attained. For example, Rhodes & Pownall (1994) measuring young glacigenic quartz samples from a range of environments in the Garwhal Himalaya observed high residual signals, specifically the presence of significant thermal transfer signals. For quartz, a broad generalization concerning grain origin can be made: Samples containing grains recently eroded from bedrock typically have low OSL sensitivity and are relatively difficult to bleach, owing to large quantities of charge in less-bleachable traps. In contrast, quartz that has experienced multiple cycles of reworking over the recent geological past, such as desert dune sands, or significant heating by wildfires or in hearths typically has high OSL sensitivity (Pietsch et al. 2008) and is more easily bleached to a low residual level.

4.3. Successful Bleaching

For successful OSL bleaching, both environmental and sample characteristics are important. **Figure 7** illustrates this interplay, showing selected environments. Several approaches to explore this issue have been adopted, both for individual samples and in building a wider understanding of different environments and contexts. These include

1. Using simple geomorphic models to reconstruct grain movement for different environments and to predict optimal bleaching regimes (e.g., Fuchs & Owen 2008),
2. The measurement of modern (recently deposited) samples from a range of contexts to assess their residual signals and apparent age (e.g., Rhodes & Bailey 1997, Singarayer et al. 2005),
3. Comparison between OSL age and independent chronological control in specific environments (e.g., Olley et al. 2004b),
4. Comparison between closely spaced OSL samples with different depositional energies, grain size, and/or mineralogy (e.g., Richards et al. 2000), and
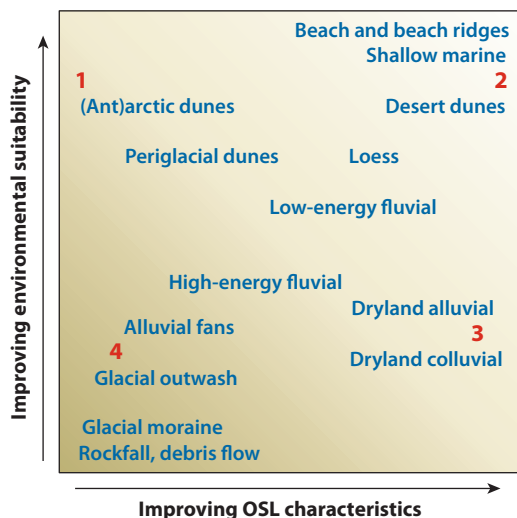5. Use of OSL signals observed during dating to help determine the completeness of bleaching.

Figure 7

The degree of bleaching achieved by quartz grains during transport is a function of both the environment and sample characteristics. Environments characterized by repeated and/or lengthy light exposure (e.g., beaches, dunes) contrast with those characterized by little light exposure (e.g., debris flows, moraine). But the environmental history of quartz grains also affects their bleaching rate. Grains recently eroded from bedrock typically bleach more slowly than those with an extended residence at the surface. Darker colors correspond to less effective bleaching. Numbers in red refer to examples highlighted in the text. OSL, optically stimulated luminescence.

In this final category, several methods have been used including (*a*) changes in OSL decay shape (Rhodes 1988; Bailey 2003) and, more importantly, (*b*) differences in D_e values between different aliquots or grains (Murray & Roberts 1997; see Section 5.5).

5. EQUIVALENT DOSE DETERMINATION

The SAR protocol has many advantages over other equivalent dose determination methods such as the multiple aliquot additive dose procedure. It is used for quartz OSL, feldspar OSL and IRSL, and also for polymineral fine-grained samples. Recent applications using TL signals adopt similar approaches.

5.1. Preheating

In D_e determination, natural OSL intensity is compared with that induced by different laboratory doses (**Figures 3** and **8**). Before each OSL measurement, the sample is preheated to remove unstable signal components induced by irradiation in order to stimulate transfer of unstable charge to OSL traps (mimicking natural dosing processes) and ensuring equal signal erosion, thus allowing comparison between measurements. As individual samples have different characteristics, distinct preheat treatments may be required for optimal age determination. A range of tests including the preheat plateau test (Murray & Wintle 2000) can be used for optimization, using a subset of samples from each suite.
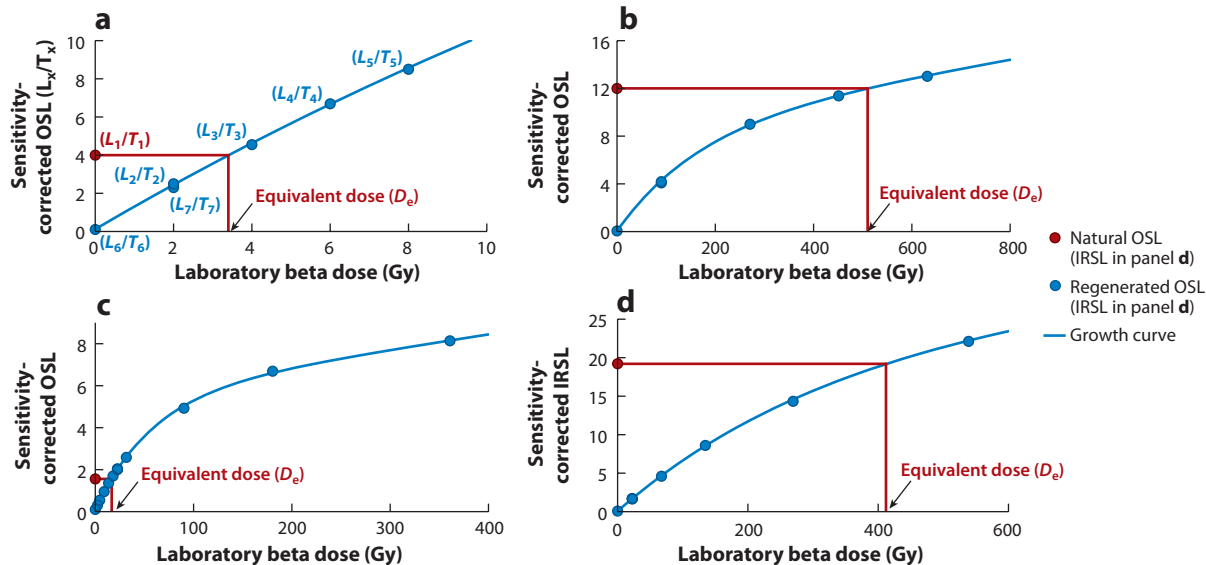
Figure 8

Optically stimulated luminescence (OSL) and infrared stimulated luminescence (IRSL) growth curves used to determine equivalent dose (D_e). (*a*) A typical single aliquot regenerative-dose (SAR) protocol comprising seven steps, in which the natural or regenerative-dose OSL (L_x) is corrected by the OSL response to a small test dose (T_x). For each aliquot, the natural OSL (L_1/T_1; *red*) is compared with the growth curve, which is defined by the regenerative-dose OSL measurements (L_2/T_2, L_3/T_3 ...; *blue*) for that aliquot, to provide the D_e estimate. (*b*) OSL response from an older quartz aliquot approaching saturation with a D_e of ~500 Gy [Gray, the SI unit of radiation dose (1 Gy = 1 J·kg^{-1})]. (*c*) OSL response of an aliquot of quartz grains from a late Pleistocene fluvial deposit with a D_e of ~16 Gy. This sample is far from saturation. (*d*) IRSL of feldspar from an older sample with a D_e of ~400 Gy. The IRSL signal shows less pronounced curvature owing to different saturation characteristics in comparison with the quartz sample in panel *c*.

5.2. Sensitivity Correction

Heating redistributes hole centers responsible for luminescence emission, changing the luminescence efficiency (Wintle & Murray 1999). The SAR protocol incorporates a direct assessment of OSL sensitivity immediately after the natural and every regenerative-dose OSL measurement (L_x). This is achieved by administering a small uniform test dose, a lower temperature preheat, and a second OSL measurement (T_x). The ratio of the background-subtracted initial OSL signal from each natural and regenerative-dose measurement to the following sensitivity measurement (L_x/T_x) is used to construct a growth curve (**Figure 8**) and determine D_e for that aliquot. Each sequence of irradiation, preheat, OSL measurement, test dose, second heat, and OSL sensitivity measurement is termed a SAR cycle. Typically six or seven cycles are performed, including a zero-dose cycle to assess thermal transfer magnitude and a repeat of the first regenerative-dose point to test successful sensitivity correction.

5.3. Recuperation and Thermal Transfer

Thermal transfer is the charge movement during heating, in this case into OSL traps from other sources. Recuperation is the special case in which charge originating in the same OSL traps was phototransferred to less stable traps by light exposure, before subsequent thermal transfer during heating (Aitken & Smith 1988). Both effects have the potential to increase D_e value. Recuperation may cause a residual signal after burial if only a brief single bleaching event was experienced. For

Growth curve: the response of the OSL signal to the applied dose

samples that suffer from thermal transfer, the use of a lower temperature preheat may mitigate the effect on D_e overestimation (Rhodes 2000). A zero-dose SAR cycle is included in dating protocols to test for thermal transfer and recuperation. Typically a fraction of 1% of the sensitivity-corrected natural OSL signal is observed.

5.4. Recycling Ratio and Dose Recovery Test

The recycling ratio is a test of the sensitivity correction procedure for each aliquot. The final regenerative dose administered is selected to be identical to the first regenerative dose given. The recycling ratio is the ratio of this final sensitivity-corrected OSL (L_7/T_7) to that of the same dose value given near the start of the measurement sequence (L_2/T_2). A ratio value of 1.0 is ideal, and values between 0.9 and 1.1 are usually considered adequate, depending on measurement uncertainties in these values.

A more substantive test of the basic SAR assumptions is the dose recovery test (Wintle & Murray 2006). This procedure complements normal dating measurements, requires additional aliquots, and takes approximately the same machine time as age estimation. For this reason, dose recovery tests are typically performed for one or a small number of samples from each suite. After zeroing the natural signal, each aliquot is administered a known laboratory dose, and a full SAR protocol measurement sequence is performed.

5.5. Detection of Incomplete Zeroing and Grain Mixing

Variation in D_e values for different aliquots indicates diverse dose values for individual constituent grains. Common causes of mixed-dose populations are (*a*) incomplete zeroing at deposition, and (*b*) postdepositional mixing of grains from different beds, for example, by bioturbation (Bateman et al. 2003). Aliquots typically comprise several hundred grains, though small aliquots of less than 100 may be employed (Olley et al. 1998). Dramatic sensitivity differences between grains allow dose variation to be observed; the OSL signal comes dominantly from a few highly sensitive grains (Rhodes 2007).

The variation between aliquots can be displayed using a radial plot (**Figure 9**) or alternative graphs. D_e variation is small when constituent grains carry the same dose. Where a substantial proportion of aliquots display variation in D_e value, the sample may be considered unsuitable for dating; or it may be modeled using a suitable statistical age model such as the minimum age model (see Section 5.6, below), or single-grain OSL measurements may be undertaken, to further delineate the causes of the observed variation.

5.6. Analysis Methods

For well-bleached samples, the central age model provides an estimate of mean dose and uncertainty, along with overdispersion, termed σ_b (Galbraith et al. 1999). Overdispersion is caused by several factors including differences in natural beta dose rates to individual grains (or beta microdosimetry; Nathan et al. 2003); high σ_b values (e.g., >10%) may indicate grain mixing or incomplete zeroing, although no single threshold value exists owing to variations in grain sensitivity distributions.

Incomplete signal zeroing often produces skewed dose distributions, with a minority of high dose estimates forming an extended high value tail. In such cases, it may be possible to extract a meaningful equivalent dose estimate using one of several statistical techniques, including the
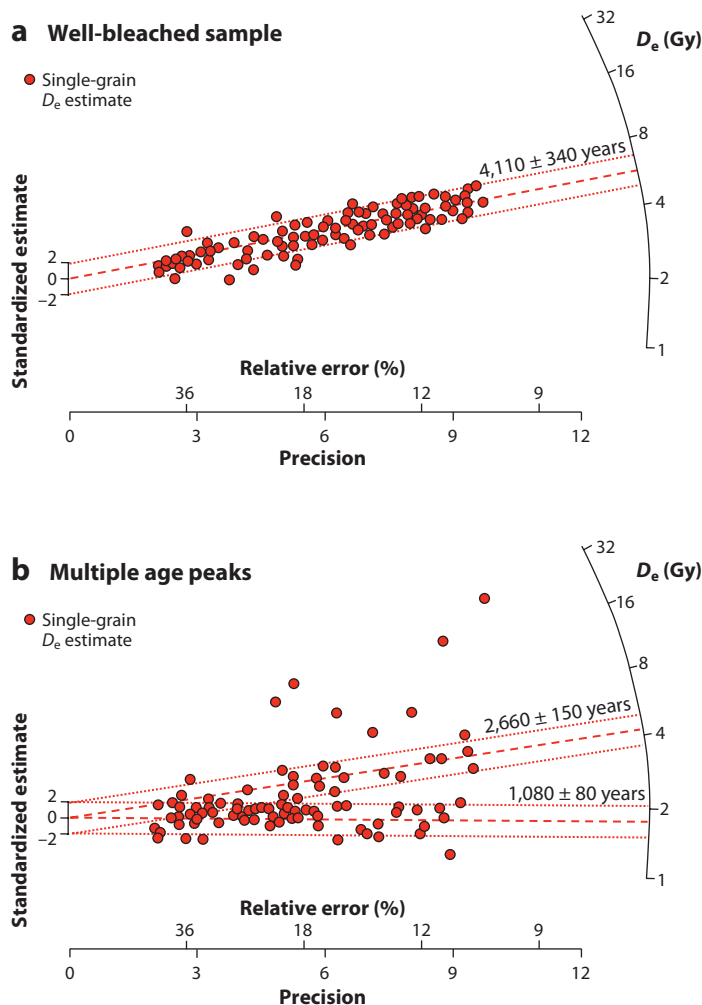
Figure 9

Radial plots of quartz single grains from two samples of young fluvial sediment from Australia. The radial plot displays useful information, but can be hard to read. The D_e for each grain is read off the plot by drawing a line from the origin (0 on the Standardized estimate axis) through the symbol (*red circle*) to the arcuate dose axis. The horizontal axis displays the relative error in the D_e estimate for that grain. (*a*) The dashed line shows the mean dose for this typical well-bleached sample (age shown above), and the dotted lines above and below represent the 2σ error limits. (*b*) This sample displays multiple dose values, and a finite mixture model was used to fit the distribution. The lower two dose components are shown by red dashed lines, with corresponding age estimates presented. Gy stands for Gray, the SI unit of radiation dose (1 Gy = 1 J·kg^{-1}).

minimum age model (MAM) developed by Galbraith et al. (1999). When variations in D_e values are observed, the inferred cause of this variation represents a hypothesis; application of the minimum age model does not necessarily provide a reliable age estimate. The use of different grain sizes (subject to different transport histories), different mineral fractions, and samples from closely spaced beds within the same sediment succession may often help resolve these questions, especially if analysis using Bayesian statistical methods is applied (Rhodes et al. 2003).

5.7. Single-Grain Optically Stimulated Luminescence

Single-grain OSL is now well established for quartz, though less exploited for feldspar grains, using a SAR protocol virtually without modification. An automated attachment for the Risø Reader has been in use for approximately one decade and is well used in paleoanthropological contexts, particularly within caves and rock shelters (e.g., Henshilwood et al. 2002, Jacobs et al. 2003, Bouzzouggar et al. 2008). This approach has been less widely adopted for routine dating of other contexts, owing primarily to the significant investment in measurement time. Where measured dose distributions contain multiple peaks, the finite mixture model of Galbraith & Green (1990) is commonly applied (**Figure 9**).

Where quartz OSL sensitivity is low, including many glacigenic and neotectonic contexts, single-grain OSL measurements are particularly inefficient and time consuming as few grains provide sufficient signal for measurement (Duller 2006). This area has great potential for future developments, and the routine use of single-grain measurements will probably increase in forthcoming years.

6. DOSE RATE DETERMINATION

An accurate estimate of the mean dose rate experienced by sample grains is required for each location. Cosmic dose contributes a small component (typically less than 10%), including a soft component when buried less than 50 cm deep and a hard component (dominantly muons) that extends down to many tens of meters. These are conventionally estimated using the equations of Prescott & Hutton (1994) and Prescott & Stephan (1982), requiring accurate measurements of overburden thickness and density besides information on past variations.

Sediment dose rate can include a component from within the grains themselves (e.g., K feldspar grains), but dominantly comes from surrounding grains. Contributions are from ^{40}K and isotopes within the decay series of ^{238}U, ^{235}U, and ^{232}Th, comprising many emissions of different type, energy, and activity. For etched grains, external alpha dose rates can be ignored; otherwise the relative efficiency of alpha irradiation (to beta and gamma) must be determined. For coarse-grained (sand-sized) samples, beta dose rates usually form the largest component (up to 3-mm range in sediment), followed by gamma (up to 30–40-cm range).

6.1. Methods Available

Sediment dose rate may be determined by measuring radioactive emissions directly or by analyzing concentrations of K, U, and Th; Adamiec & Aitken (1998) provide energy conversion values. Gamma spectrometry can be performed using high-resolution laboratory Ge detectors, providing U-series disequilibrium measurements, or using a portable low-resolution NaI spectrometer during collection. Several different systems can be used to count beta decays directly. Thick source alpha counting of emissions from U and Th (but not K) is relatively inexpensive, but slow and arduous; it is useful for fine-grained samples where alpha dose rate is important.

Concentrations of U, Th, and K may be determined using a variety of methods. INAA (instrumental neutron activation analysis) measures U and Th directly, as well as K. X-ray fluorescence may be used for K concentration, but is rarely sufficiently sensitive for U and Th at typical sediment values. ICP (induction coupled plasma)–MS (mass spectrometry) is useful for U and Th concentrations, whereas ICP-OES (optical emission spectrometry) is generally used for K, or the older method of flame photometry. The sample must be fully dissolved before analysis commences (often difficult to achieve), and the degree to which the sample is representative of the whole

sediment must be considered, particularly for gamma dose rate. No information is forthcoming with respect to disequilibrium using concentration techniques alone.

6.2. Dose Rate Attenuation

For beta radiation, attenuation across individual grains must be calculated, using different values for K, U, and Th (assuming equilibrium for U and Th) that vary with grain size (Mejdahl 1979, Aitken 1985). Water contained within sediment pores absorbs radiation, and a single correction to each different form of radiation (alpha, beta, and gamma) is typically employed, based on the measured water content. The total dose rate for sand-sized grains typically varies by ∼1% for a 1% change in water content. For fine-grained samples and sediments such as deep marine deposits, this is an important consideration, and more complex water content modeling may be required.

6.3. Uranium Disequilibrium

Secular disequilibrium is rare for the Th decay series, but not uncommon at modest scales for U daughter isotopes, particularly in environments with relatively unweathered parent material (Olley et al. 1996). It is important that this effect is assessed at least for some samples within each suite, either using high-resolution Ge gamma spectrometry measurements in the laboratory or a first-order assessment comparing the top of the U decay series (e.g., by INAA or ICP-MS) with the bottom (e.g., U content determined using ^{214}Bi by in situ NaI gamma spectrometry).

In summary, more than one method of dose rate determination is preferable, and the sample size or scale of measurement should reflect the scale of radiation. Some means to assess U series disequilibrium is important, and careful consideration of water content and overburden variations must be made.

7. APPLICATIONS

The range of contexts dated by OSL has increased rapidly over the past decade and is now extensive (**Figure 1**). Applications started with archaeological and eolian contexts (Rhodes 1988, Smith et al. 1990), and fluvial and glacigenic environments (Perkins & Rhodes 1994, Owen et al. 1997) were tackled as bleaching problems were better understood. **Table 1** presents a range of OSL applications, from geologic to archaeological, and lists specific environments and sedimentary contexts where dating is now performed. Recent useful reviews with details of specific environments have been produced by Rittenour (2008; fluvial and neotectonic contexts) and Fuchs & Owen (2008; glacigenic sediments).

The resolution (± 5 to 10% at 1σ) and age range (1 to ∼200,000 years) render OSL well suited for the study of recent phenomena with event resolutions of several years, Holocene events on timescales of hundreds of years, and particularly for events within the last glacial cycle with characteristic timescales of thousands of years. The specific advantages for dating sediment offered by OSL in comparison with other techniques is that zeroing has a direct relationship to the depositional event and that the target material is the sediment itself.

7.1. Technique Reliability

Murray & Olley (2002) assessed the performance of quartz SAR OSL in comparison with independent methods for 53 samples, updated recently by Rittenour (2008), finding excellent agreement (**Figure 10**). Rhodes et al. (2003) optimized quartz SAR precision for several archaeological

Table 1 Applications and sedimentary environments for OSL dating, with comments on degree of establishment with limitations and specific contexts dated

Applications	Comments	Contexts
Tectonic and paleoseismic	Relatively recently applied	Marine, fluvial, lacustrine, slope deposits
Paleoclimatic and paleoenvironmental	Now widely used	Wide range of sediments
Geomorphic and Quaternary	Now widely used	Wide range of sediments
Environmental and process studies	Relatively recently applied	Soils, fluvial, potential for wider range
Archaeological and paleoanthropological	Now widely used	Fluvial, colluvial, soils, heated/fired materials
Environments		
Eolian (wind transported)	Usually successful	Sand dunes, loess
Fluvial, alluvial, lacustrine (water-lain)	Zeroing can be problematic	River terraces, alluvial fans, flood plains, lakes
Marine: coastal and offshore	Zeroing issue in deep water	Raised beaches, beach ridges, deeper water
Glacigenic	Zeroing and characteristics can be problematic	Moraine and till, outwash, glaciomarine
Slope deposits	Zeroing and characteristics can be problematic	Colluvium, rockfall, debris flows
Caves (karstic)	Zeroing can be problematic	Shallow cave sediments, sands and silts
Anthropomorphic	Zeroing can be problematic	Artificial fill, anthropomorphic soils
Volcanic rocks, precipitation	Characteristics are often problematic	Opal, biogenic opal, phenocrysts, xenocrysts
Soils	Grain movement studies	Modern, compound and buried soils
Heated materials	Usually successful	Ceramics, wild fires, thermochronology
Strained and shocked materials	Little research to date	Impact craters, fault movement

sediments achieving ±1–2% at 1σ and demonstrated agreement with AMS ^{14}C dates on burnt seeds with no measureable systematic error (**Figure 11**). For highly insensitive quartz samples, the origin and thermal stability of OSL signals are not clear and reliability is not assured. Age comparison studies for feldspar are less well developed; relationships to radiocarbon and quartz OSL ages suggest that fading corrections can work successfully (e.g., Davids et al. 2010).

7.2. Eolian Sediments

Many researchers have studied the timing of dune construction using OSL; the technique is ideally suited for this task and is making a highly significant contribution to our understanding of these widespread landforms and arid zone sediment mobility. Recent approaches focus on the collection of multiple samples at different depths from cores within dunes. Stone & Thomas (2008) found deposition throughout the past 100,000 years in the southern Kalahari, whereas Fitzsimmons et al. (2007) demonstrated a pronounced pulsing of dune deposition within central Australia on similar timescales. Fujioka et al. (2009) used OSL to demonstrate the stability and great antiquity of individual longitudinal dunes from the Simpson Desert and used OSL ages to constrain a dune construction model to determine cosmogenic burial age estimates; and for the first time, this provided an age estimate for the age of a dunefield, besides its constituent dunes (**Figure 12**). Bristow et al. (2010) overcame problems of very low quartz sensitivity using novel analysis methods to date reversing dunes in Antarctica on timescales of centuries to millennia (1 on **Figure 7**), drawing parallels with dunes on Mars.

Loess deposits were widely dated by TL, but OSL and IRSL are now routinely applied. Fine grains are commonly used, either polymineral or by enriching quartz using H_2SiF_6 treatment. In
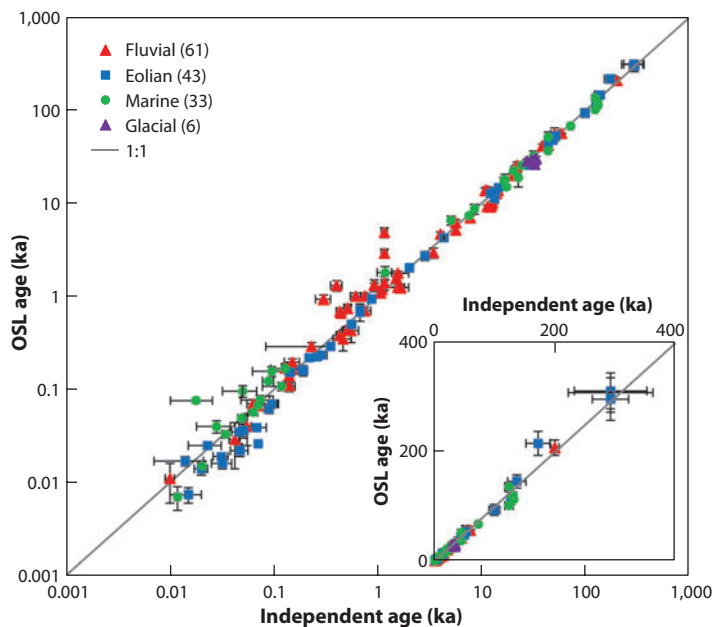
Figure 10

Comparison between optically stimulated luminescence (OSL) age and independent chronological control for 143 samples from fluvial, eolian, marine, and glacial contexts, measured using quartz single aliquot regenerative-dose determinations. The solid line shows agreement between methods, and uncertainites represent 1σ. Data are from Murray & Olley (2002) and Rittenour (2008). There is good agreement, although several samples lie above the line; they are interpreted as representing the effects of incomplete bleaching of the OSL signal. Inset figure shows the same data using linear axes.

some locations, fine sand-sized quartz can be isolated. Owing to high dose rates, conventional OSL is usually limited to the last glacial cycle. Patterns of pulsed loess deposition are emerging, throwing light on previously unrecognized hiatuses and improving climatic interpretations (Stevens et al. 2007).

7.3. Marine and Lacustrine Deposits

Repeated reworking of grains by wave action makes beaches, beach ridges, and shallow marine sediments well suited for OSL. Several Holocene beach ridge sequences have been dated with good internal and external agreement, and Pleistocene raised beach sequences are also successful targets (e.g., Rhodes et al. 2006; **Figure 13**). Nielsen et al. (2006) report ages as young as 10 ± 2, 8.8 ± 0.9, and 5.0 ± 1.0 years for a Danish dune ridge, part of a sequence of 163 ridges that span the past 9,000 years, whereas Nott et al. (2009) dated 28 samples from 29 ridges in NE Queensland, Australia, finding that Holocene cyclone activity was significantly greater than projected from the local short historical record (2 on **Figure 7**). Studies of Tsunami deposits show great potential for improving hazard assessments in populated areas with poor or absent historical records (e.g., Murari et al. 2007). Olley et al. (2004a) used single-grain quartz OSL to date deep marine sediments; though problematic for bleaching, OSL studies have great potential within this environment.

Dating of lakes, both shorelines and basal sediments, is now widespread. Magee et al. (2004) controlled the timing of huge lakes in central Australia over the past 125,000 years, and many
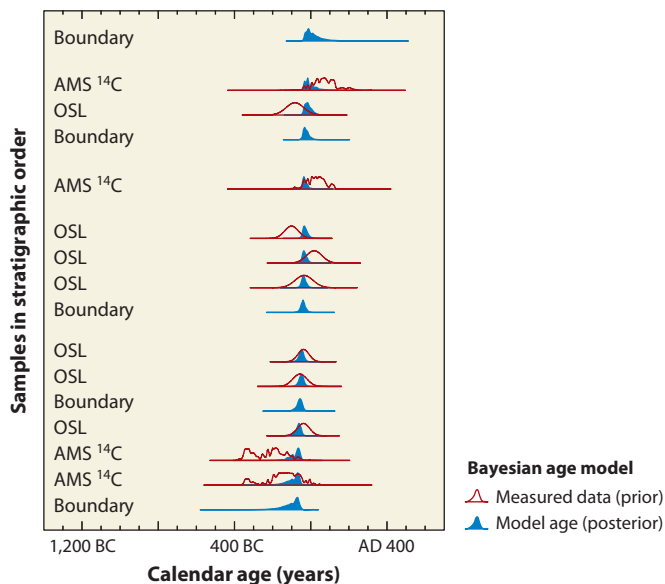
Figure 11

Testing the performance of the quartz single aliquot regenerative-dose protocol. A sequence of seven optically stimulated luminescence (OSL) samples interstratified with burnt seeds dated by AMS ^{14}C from ~2,000-year-old archaeological deposits from Old Scatness, Shetland, UK, were dated, optimizing parameters to maximize measurement precision. Open symbols show measured age-probability plots for each ^{14}C and OSL sample displayed in stratigraphic order. The consistency of all the age estimates was tested using Bayesian statistical methods, which demonstrated that there was no measureable systematic error in the OSL ages. The Bayesian procedure uses the stratigraphic information to constrain the age estimates at each position and provide an improved age determination, shown by the solid samples. Details of samples and procedures are provided by Rhodes et al. (2003) (click on the PDF version of the figure to view the original source article).

recent studies have focused on Tibet and China. Information regarding monsoon intensity and penetration, besides dating stratified paleoenvironmental records, provides valuable contributions.

7.4. Fluvial and Alluvial Sediments

Application to flights of fluvial terraces has changed the interpretation of many of these important landforms; though previous interpretations stressed the role of sea-level fluctuations and

Figure 12

Combined optically stimulated luminescence (OSL) and cosmogenic burial age estimates for longitudinal dunes from the Simpson Desert, Northern Territory, Australia. (*a*) The map shows the large counterclockwise whorl of longitudinal dunes around central Australia, marking ancient wind directions. (*b*) The photograph shows sample collection using 6-cm-diameter steel tubes inserted through a hollow sand auger down to 12 m using a truck-mounted drill rig. (*c*) The cross section displays age estimates (OSL in *red*, cosmogenic data in *blue*) from three cores in a single dune at Minga South. OSL reaches saturation at approximately 200,000 years. Also shown are ancient dune surface profiles, marked by paleosols with sharp textural changes, demonstrating long-period stability of the dune location. (*d*) The satellite image shows the pattern of dunes in the region, along with sampling locations (image provided through NASA's Scientific Data Purchase Project and produced under NASA contract by Earth Satellite Corporation). Cosmogenic data provide an age estimate for dunefield initiation, whereas OSL dates the last movement. Details can be found in Fujioka et al. (2009) (click on the PDF version of the figure to view the original source article).
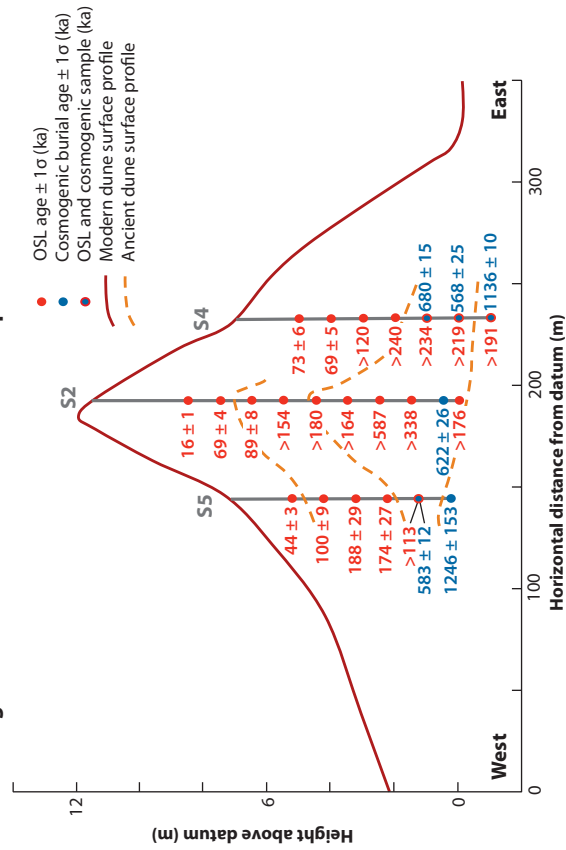
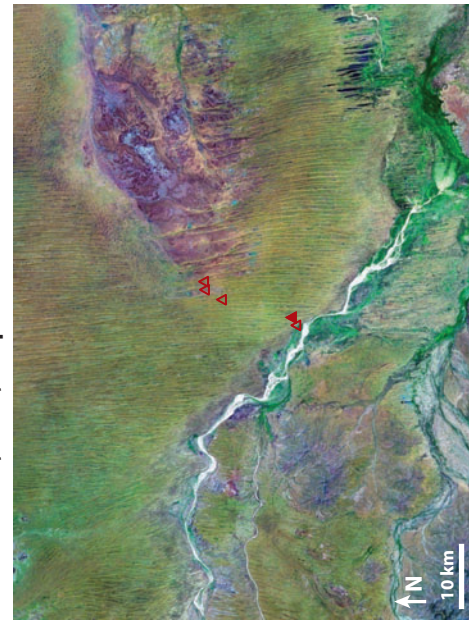**a Australia: mainland with longitudinal dunes**

Not to scale

★ New Crown, Finke, Northern Territory

↑ Paleo wind direction inferred from dunes

b Sample collection

6-cm-diameter sampling tube

d New Crown, Finke, Simpson Desert

▲ Minga South dune (results shown in panel **c**)
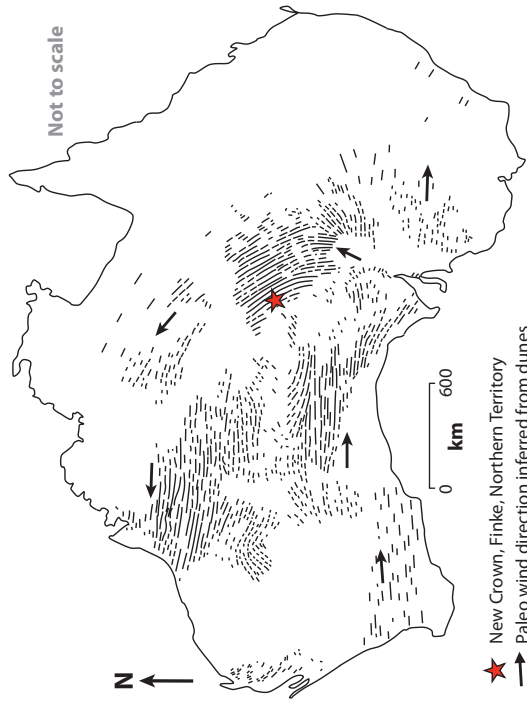
△ Other locations (results not shown)

c Minga South dune: cross section and sample locations

● OSL age ± 1σ (ka)

● Cosmogenic burial age ± 1σ (ka)

● OSL and cosmogenic sample (ka)

— Modern dune surface profile

— Ancient dune surface profile

S5: 44 ± 3, 100 ± 9, 188 ± 29, 174 ± 27, >113, 583 ± 12, 1246 ± 153

S2: 16 ± 1, 69 ± 4, 89 ± 8, >154, >180, >164, >587, >338, 622 ± 26, >176

S4: 73 ± 6, 69 ± 5, >120, >240, >234, 680 ± 15, >219, 568 ± 25, >191, 1136 ± 10

West · East

Height above datum (m) · 12 · 6 · 0

Horizontal distance from datum (m) · 0 · 100 · 200 · 300
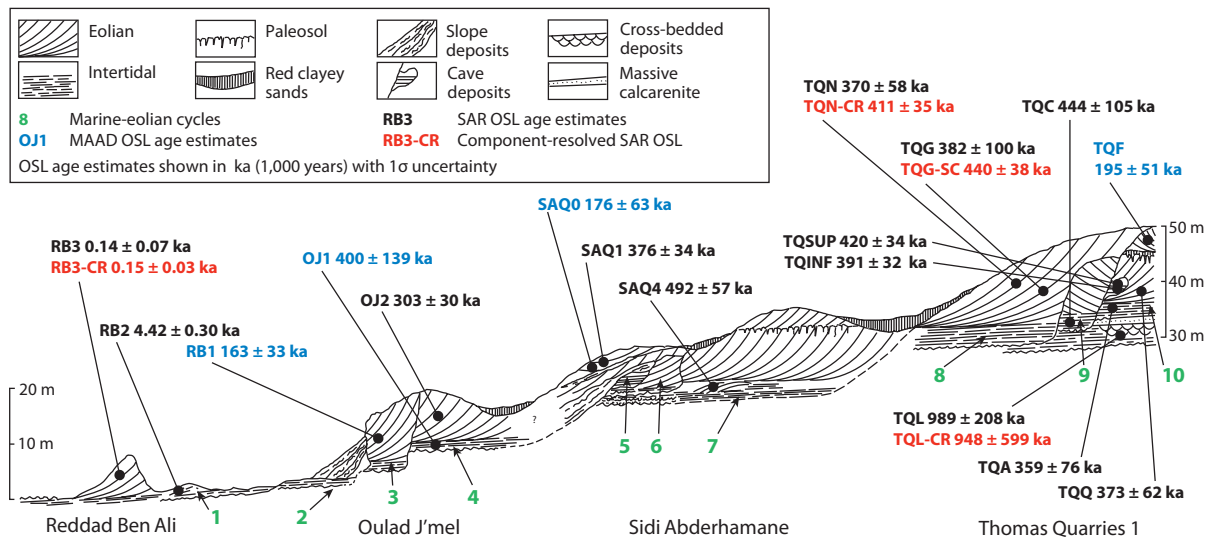
Figure 13

Optically stimulated luminescence (OSL) dating of an impressive Pleistocene raised beach and eolianite sequence, Casablanca, Morocco. Conventional quartz OSL using single aliquot regenerative-dose (SAR) (in *black*) and multiple aliquot additive dose (MAAD) (in *blue*) is complemented by novel slow component (SC) and component-resolved (CR) OSL data, with age estimates back to approximately 1,000,000 years. For MAAD data and some older SAR data, uncertainties are large. Based on results of Rhodes et al. (2006) but including newly measured data (click on the PDF version of the figure to view the original source article). Abbreviations: OJ, Oulad J'mel; RB, Reddad Ben Ali; SAQ, Sidi Abderhamane; TQ, Thomas Quarries.

100,000-year glacial cycles in their formation, direct dating highlights the importance of shorter climate fluctuations, such as those associated with Heinrich events (Lewis et al. 2009). Terrace systems of many of the world's major rivers have been dated using OSL, including the Mississippi and Colorado (USA), Loire (France), Rhine (Germany, Netherlands), Danube (Austria), Jena (Russia), Amazon (Brazil), Thames and Solent (UK), Murrumbidgee and Lachlan (Australia), Yellow (China), and Tejo (Portugal), clarifying local, regional, and global climate and sediment supply controls. An impressive body of data from the Rhine delta in the Netherlands allows processes taking place over decades to glacial cycles to be traced, providing information for flood risk assessment and a better understanding of climate changes within the catchment of this important river (Wallinga et al. 2010). Although dating in fluvial contexts can be problematic, owing to low quartz sensitivity and incomplete zeroing issues, dense sampling strategies and use of single-grain OSL are providing solutions. Murton et al. (2010) used OSL and ^{14}C to constrain the age of massive flood events in Arctic Canada, tracing the outflow route from Lake Agassiz, during the Younger Dryas cold event.

Smaller fluvial systems are equally suitable for OSL, when tackled appropriately. Issues of incomplete zeroing are common but manageable. Landscape stability, geomorphic change, and climate records may be extracted from these archives using suitable dating procedures (e.g., Rodnight et al. 2006, Arnold et al. 2007). Rhodes et al. (2010) dated approximately 50 samples from a single catchment in arid New South Wales (3 on **Figure 7**) using quartz single grains, finding that multiple peaked age distributions were common (**Figure 9**), but that internal consistency of age estimates was high.

7.5. Glacigenic Contexts

Direct dating of glacigenic deposits and outwash terraces has highlighted the importance of shorter period glacial events in contrast to global scale events on 100,000-year glacial cycles, and the importance of asynchronous glaciation between the Laurentide Ice Sheet and glaciations in Antarctica (Gore et al. 2001), the Himalayas (Owen et al. 1997, Richards et al. 2000) and the Pyrenees (Lewis et al. 2009). The double whammy of rapid deposition along with poor quartz characteristics (4 on **Figure 7**) makes these deposits challenging to date but has been a driver of technical innovation for OSL. This application is particularly valuable when combined with cosmogenic nuclide dating of moraines (e.g., Spencer & Owen 2004).

7.6. Tectonic Applications

Use of OSL to understand neotectonic processes and rates has great potential and generally represents special cases of other applications, in particular fluvial and colluvial sediments. Samples are typically from tectonically disturbed or translated sediments or those formed in response to fault rupture (sag ponds, small fans). Similar issues to those encountered in glacigenic contexts are frequently encountered (e.g., Fattahi et al. 2010). Experience from other contexts with some similarities (e.g., ditch-fill sediments) suggests significant future developments, particularly making use of single grains and K feldspar for young events. When linked to dating of geomorphic features, OSL can help unravel the complex relationships between climate, tectonics, and landscape development.

7.7. Other Applications and Contexts

Perhaps surprisingly, quartz OSL does not work well when applied to volcanic contexts. Although age estimates may in some cases be derived, characteristics of volcanic quartz are generally not well suited for OSL, though red TL emissions appear reliable (Westaway 2009).

Colluvial sediments and cave deposits have been studied in archaeological applications and, despite significant bleaching issues, can provide good agreement with other techniques using appropriate OSL methods, in particular single grains. Rather few studies of bioturbation (Bateman et al. 2003) and grain mobility have been performed, despite the great potential of OSL for this area. Heimsath et al. (2002) used quartz single-grain OSL combined with in situ cosmogenic isotope production to model soil development and creep rate in Australia.

8. NEW AND ONGOING DEVELOPMENTS

Many exciting new developments are currently being actively researched. These include OSL age range extension to greater than 1,000,000 years, OSL thermochronology, pulsed OSL/IRSL for improved signal differentiation, portable OSL/IRSL units for rapid field assessment and planetary applications, and spatial imaging using OSL.

8.1. Age Range Extension

Dose saturation imposes an upper limit to all forms of luminescence dating (**Figure 8b,c**). In rare situations, conventional quartz OSL can provide age estimates close to 1 Ma (Rhodes et al. 2006; **Figure 13**). Singarayer et al. (2000) demonstrated the potential for using the less bleachable slow components of quartz OSL with high dose saturation levels to extend the age range. They

may be deconvoluted using linear modulation OSL (LM-OSL) (Bulur 1996) or a mathematical transformation termed pseudo LM-OSL (Singarayer & Bailey 2003).

Rhodes et al. (2006) used both conventional quartz OSL and slow-component OSL to date samples of raised beach and eolianite from an impressive succession at Casablanca, Morocco (**Figure 13**). These sediments contain hominid material, Palaeolithic archaeology, a single U-series age estimate, and ESR dates; Bayesian statistical techniques demonstrated high overall consistency. The wider applicability of slow components has yet to be demonstrated.

Wang et al. (2007) have proposed an alternative method to access deep traps using quartz thermal-transfer OSL (TT-OSL), and preliminary assessments by numerous workers are highly encouraging (e.g., Porat et al. 2009), providing preliminary age estimates in the range of 40,000 to 1 million years. Jain (2009) used high-energy violet photons (3.06 eV) to stimulate OSL from deep traps with promising results. Isothermal TL of quartz using a SAR protocol and the red TL quartz signal show promise, with signals that grow to high doses, which is important for age range extension. At present, these techniques should be considered experimental, but a significant research effort is currently underway to better define reliable protocols and sample suitability.

8.2. Thermochronology and Paleothermometry

Raised temperatures allow charge to escape from traps, but as rocks cool during exhumation, traps start to retain charge. Trap parameters (the trap depth, E_α, and escape frequency factor, s) are well-established for quartz OSL fast component (e.g., Murray & Wintle 2000; Singarayer & Bailey 2003), allowing this process to be modeled as a function of dose rate and cooling rate. The low blocking temperature ($\sim$30°C–35°C) provides access to examine erosion processes on timescales of 10,000 to 100,000 years. Herman et al. (2010) applied this approach to investigate erosion rates in the Southern Alps, New Zealand. Using OSL age estimates for 13 metasandstone samples from a topographic profile, they applied a mathematical inversion to solve for relief change and exhumation rate, finding a value consistent with the longer term rate assessed using (U-Th)/He and fission track. They demonstrated that over the last glacial cycle, relief change has been limited (despite 800 m of erosion), even during switches between glacial and fluvial denudation, suggesting that the landscape has achieved steady state.

The technique has great potential to address problems of erosion rate in high mountain and tectonically active environments but requires further fundamental research before becoming routine. Many quartz samples in these environments have low fast component sensitivity, and greater uncertainty accompanies the origin and behavior of other components. Preliminary measurements of feldspar OSL and IRSL show great promise, though increased complexity of the OSL/IRSL system may slow development.

OSL and IRSL signals are zeroed by heating, providing a means to date wildfire events. When combined with TL measurements, which may be used to assess maximum temperature, both the time and severity of burn events may be determined. Combined single-grain OSL and TL determinations provide exciting possibilities for improving understanding of fire ecology and hazard prediction. There is also significant potential for low-temperature paleothermometry on planets and planetoids.

8.3. Pulsed Optically Stimulated Luminescence

When stimulating light is switched on only briefly (tens of microseconds) in OSL and IRSL, both signal build-up and subsequent decay have timescales (1 μs to tens of microseconds) characteristic of different sources. This approach may be used to differentiate between quartz and feldspar

OSL signals (Denby et al. 2006) and to better understand trap structures within individual minerals. The potential for improving the distinction of signals from different minerals is exciting and presents the possibility of achieving mineral-specific measurements without requiring prior mineral separation. This method is not yet routine and generally significantly reduces signal-to-noise levels and therefore is unlikely to be used where OSL sensitivity is low. It provides a useful tool for exploring underlying physical mechanisms (e.g., Chithambo et al. 2008), besides offering opportunities to make OSL and IRSL measurements in situ.

8.4. Portable Optically Stimulated Luminescence and Planetary Applications

Equipment initially designed for food irradiation studies has been modified in order to allow OSL and IRSL to be measured away from the laboratory. This has been used in a range of archaeological and geologic applications to assess suitable locations for conventional OSL/IRSL dating, to identify sharp steps in age-depth profiles, and to undertake process studies (Sanderson & Murphy 2010).

As sample sensitivities vary, natural OSL (or IRSL) intensity does not directly relate to age. Dating awaits the development of a safe and convenient X-ray source that can be incorporated into portable equipment, along with a preheating facility, to allow approximate age estimation to be undertaken in the field (dose rates may be assessed using a portable NaI gamma spectrometer). Such equipment is currently being developed for use on Mars (Jain et al. 2006), in order to study the age structure of dunes and apparent fluvial deposits, but also has great potential for terrestrial applications. Miniaturized versions might be used in rapid down-core age assessment or mineral characterization, for example.

8.5. Luminescence Imaging

Several systems have been developed to allow relatively low-resolution TL imaging using an imaging photon device, essentially an array (e.g., 256×256) of miniature photomultiplier tubes. Spatial resolution has recently been developed for OSL to help resolve issues of bleaching and dose rate variation (Greilich & Wagner 2006). New systems, including the use of a confocal microscope, are currently in development, and spatially resolved OSL on the micrometer scale will provide insight into luminescence processes and mineral histories.

9. SUMMARY AND CONCLUSIONS

In summary, OSL dating is undergoing rapid development—although the quartz SAR protocol in particular provides reliable age estimates for sediment deposition in many contexts—and is now widely applied. Single-grain OSL measurement overcomes many problems of incomplete signal zeroing and grain mixing, and with the application of suitable dose rate methods, including an assessment of U-series disequilibrium, the technique can provide highly robust age estimates for a wide range of terrestrial surface depositional environments. Equipment for future extraterrestrial application is in development. Where one approach encounters problems (e.g., low quartz OSL signal intensity), other minerals and stimulation wavelengths may be selected. The dating materials, silt to sand-sized grains of quartz and feldspar, are virtually ubiquitous at Earth's surface. Novel applications such as low-temperature thermochronology are emerging, and other new avenues are currently being explored to extend the scope, age range, and accuracy of the method across the earth and planetary sciences.

SUMMARY POINTS

1. OSL is now widely used to date sediments spanning 1–200,000 years in age.

2. The OSL signal is sensitive to brief daylight exposure or heating.

3. Several related methods may be applied to quartz or feldspar.

4. The SAR protocol for quartz stands out as precise and accurate.

5. Single-grain OSL can overcome many previous limitations posed by incomplete bleaching.

6. Applications cover many Earth surface environments and are being extended by current research.

7. Future planetary applications are already being investigated and equipment developed.

8. Exciting new advances including low-temperature thermochronology and age range extension are in development.

DISCLOSURE STATEMENT

The author is not aware of any affiliations, memberships, funding, or financial holdings that might be perceived as affecting the objectivity of this review.

ACKNOWLEDGMENTS

LITERATURE CITED

Adamiec G, Aitken MJ. 1998. Dose-rate conversion factors: new data. *Ancient TL* 16:37–50

Aitken MJ. 1985. *Thermoluminescence Dating*. London: Academic

Aitken MJ. 1998. *An Introduction to Optical Dating*. Oxford: Oxford University Press

Aitken MJ, Smith BW. 1988. Optical dating: recuperation after bleaching. *Quat. Sci. Rev.* 7:387–93

Arnold LJ, Balley RM, Tucker GE. 2007. Statistical treatment of fluvial dose distributions from southern Colorado arroyo deposits. *Quat. Geochronol.* 2:162–67

Auclair M, Lamothe M, Huot S. 2003. Measurement of anomalous fading for feldspar IRSL using SAR. *Radiat. Meas.* 37:487–92

Bailey RM. 2003. Paper I: The use of measurement-time dependent single-aliquot equivalent-dose estimates from quartz in the identification of incomplete signal resetting. *Radiat. Meas.* 37:673–83

Bailey RM, Smith BW, Rhodes EJ. 1997. Partial bleaching and the decay form characteristics of quartz OSL. *Radiat. Meas.* 27:123–36

Bateman MD, Frederick CD, Jaiswal MK, Singhvi AK. 2003. Investigations into the potential effects of pedoturbation on luminescence dating. *Quat. Sci. Rev.* 22:1169–76

Bøtter-Jensen L, Duller GAT, Murray AS. 2000. Advances in luminescence measurement systems. *Radiat. Meas.* 32:523–28

Bouzouggar A, Barton N, Vanhaeren M, d'Errico F, Collcutt S, et al. 2007. 82,000-year-old shell beads from North Africa and implications for the origins of modern behaviour. *Proc. Natl. Acad. Sci. USA* 104:9964–69

Bristow CS, Augustinus PC, Wallis IC, Jol HM, Rhodes EJ. 2010. Investigation of the age and migration of reversing dunes in Antarctica using GPR and OSL, with implications for GPR on Mars. *Earth Planet. Sci. Lett.* 289:30–42

Provides a good general introduction to theory and background.

Bulur E. 1996. An alternative technique for optically stimulated luminescence (OSL) experiment. *Radiat. Meas.* 26:701–9

Chithambo ML, Ogundare FO, Feathers J, Hong DG. 2008. On the dose-dependence of luminescence lifetimes in natural quartz. *Radiat. Eff. Defects Solids* 163:945–53

Davids F, Duller GAT, Roberts HM. 2010. Testing the use of feldspars for optical dating of hurricane overwash deposits. *Quat. Geochronol.* 5:125–30

Denby PM, Bøtter-Jensen L, Murray AS, Thomsen KJ, Moska P. 2006. Application of pulsed OSL to the separation of the luminescence components from a mixed quartz/feldspar sample. *Radiat. Meas.* 41:774–79

Duller GAT. 2006. Single grain optical dating of glacigenic deposits. *Quat. Geochronol.* 1:296–304

Duller GAT. 2008. *Luminescence Dating: Guidelines in Using Luminescence Dating in Archaeology.* Swindon: English Heritage

Fattahi M, Nazari H, Bateman MD, Meyer B, Sebrier M. 2010. Refining the OSL age of the last earthquake on the Dheshir fault, Central Iran. *Quat. Geochronol.* 5:286–92

Fitzsimmons KE, Rhodes EJ, Magee JW, Barrows TT. 2007. The timing of dune activity in the Strzelecki and Tirari Deserts, Australia. *Quat. Sci. Rev.* 26:2598–616

Fuchs M, Owen LA. 2008. Luminescence dating of glacial and associated sediments: review, recommendations and future directions. *Boreas* 37:636–59

Fujioka T, Chappell J, Fifield LK, Rhodes EJ. 2009. Australian desert dune fields initiated with Pliocene-Pleistocene global climatic shift. *Geology* 37:51–54

Galbraith RF, Green PF. 1990. Estimating the component ages in a finite mixture. *Nucl. Tracks Radiat. Meas.* 17:196–206

Galbraith RF, Roberts RG, Laslett GM, Yoshida H, Olley JM. 1999. Optical dating of single and multiple grains of quartz from Jinmium rock shelter, northern Australia: Part I. Experimental design and statistical models. *Archaeometry* 41:339–64

Godfrey-Smith DI, Huntley DJ, Chen WH. 1988. Optical dating studies of quartz and feldspar sediment extracts. *Quat. Sci. Rev.* 7:373–80

Gore DB, Rhodes EJ, Augustinus PCG, Leishman MR, Colhoun EA, et al. 2001. Bunger Hills, East Antarctica: ice free at the Last Glacial Maximum. *Geology* 29:1103–6

Greilich S, Wagner GA. 2006. Development of a spatially resolved dating technique using HR-OSL. *Radiat. Meas.* 41:738–43

Heimsath AM, Chappell J, Spooner NA, Questiaux DG. 2002. Creeping soil. *Geology* 30:111–14

Henshilwood CS, d'Errico F, Yates R, Jacobs Z, Tribolo C, et al. 2002. Emergence of modern human behavior: Middle Stone Age engravings from South Africa. *Science* 295:1278–80

Herman F, Rhodes EJ, Braun J, Heinihger J. 2010. Glacial erosion equals fluvial erosion in a very active orogen, as revealed from OSL-thermochronology. *Earth Planet. Sci. Lett.* 297:183–89

Huntley DJ, Godfrey-Smith DI, Thewalt MLW. 1985. Optical dating of sediments. *Nature* 313:105–7

Huntley DJ, Lamothe M. 2001. Ubiquity of anomalous fading in Kfeldspars, and measurement and correction for it in optical dating. *Can. J. Earth Sci.* 38:1093–106

Hütt G, Jaek I, Tchonka J. 1988. Optical dating: K-feldspars optical response stimulation spectra. *Quat. Sci. Rev.* 7:381–85

Itoh N, Stoneham D, Stoneham AM. 2002. Ionic and electronic processes in quartz: mechanisms of thermo-luminescence and optically stimulated luminescence. *J. Appl. Phys.* 92:5036–44

Jain M. 2009. Extending the dose range: probing deep traps in quartz with 3.06 eV photons. *Radiat. Meas.* 44:445–52

Jain M, Anderson CE, Bøtter-Jensen L, Murray AS, Haack, et al. 2006 Luminescence dating on Mars: OSL characteristics of Martian analogue materials and GCR dosimetry. *Radiat. Meas.* 41:755–61

Jacobs Z, Duller GAT, Wintle AG. 2003. Optical dating of dune sand from Blombos Cave, South Africa: II—single grain data. *J. Hum. Evol.* 44:613–25

Lewis CJ, McDonald EV, Sancho C, Peña JL, Rhodes EJ. 2009. Climatic implications of correlated Upper Pleistocene glacial and fluvial deposits on the Cinca and Gállego Rivers, NE Spain. *Glob. Planet. Change* 67:141–52

Provides an up-to-date, nonspecialist introduction; available online.

Provides a complete survey of OSL dating of glacigenic contexts and issues.

Persists as the original concise paper on optical dating, containing many key concepts.

Magee JW, Miller GH, Spooner NA, Questiaux D. 2004. Continuous 150 ky monsoon record from Lake Eyre, Australia: insolation-forcing implications and unexpected Holocene failure. *Geology* 32:885–88

Martini M, Fasoli M, Galli A. 2009. Quartz OSL emission spectra and the role of [AlO$_4$]° recombination centres. *Radiat. Meas.* 44:458–61

Mejdahl V. 1979. Thermoluminescence dating: beta-dose attenuation in quartz grains. *Archaeometry* 21:61–72

Murari MK, Achyuthan H, Singhvi AK. 2007. Luminescence studies on the sediments laid down by the December 2004 tsunami event: prospects for the dating of palaeo tsunamis and for the estimation of sediment fluxes. *Curr. Sci.* 92:367–71

Murray AS, Olley JM. 2002. Precision and accuracy in the optically stimulated luminescence dating of sedimentary quartz: a status review. *Geochronometria* 21:1–16

Murray AS, Roberts RG. 1997. Determining the burial time of single grains of quartz using optically stimulated luminescence. *Earth Planet. Sci. Lett.* 152:163–80

Murray AS, Wintle AG. 2000. Luminescence dating of quartz using an improved single-aliquot regenerative-dose protocol. *Radiat. Meas.* 32:57–73

Murray AS, Wintle AG. 2003. The single aliquot regenerative dose protocol: potential for improvements in reliability. *Radiat. Meas.* 37:377–81

Murton JB, Bateman MD, Dallimore SR, Teller JT, Yang Z. 2010. Identification of Younger Dryas outburst flood path from lake Agassiz to the arctic Ocean. *Nature* 464:740–43

Nathan RP, Thomas PJ, Jain M, Murray AS, Rhodes EJ. 2003. Environmental dose rate heterogeneity of beta radiation and its implications for luminescence dating: Monte Carlo modelling and experimental validation. *Radiat. Meas.* 37:305–13

Nielsen A, Murray AS, Pejrup M, Elberling B. 2006. Optically stimulated luminescence dating of a Holocene beach ridge plain in Northern Jutland, Denmark. *Quat. Geochronol.* 1:305–12

Nott J, Smithers S, Walsh K, Rhodes EJ. 2009. Sand beach ridges record 6000 year history of extreme tropical cyclone activity in northeastern Australia. *Quat. Sci. Rev.* 28:1511–20

Olley J, Caitcheon G, Murray AS. 1998. The distribution of apparent dose as determined by optically stimulated luminescence in small aliquots of fluvial quartz: implications for dating young sediments. *Quat. Sci. Rev.* 17:1033–40

Olley JM, De Deckker P, Roberts RG, Fifield LK, Yoshida H, Hancock G. 2004a. Optical dating of deep-sea sediments using single grains of quartz: a comparison with radiocarbon. *Sedim. Geol.* 169:175–89

Olley JM, Murray AM, Roberts RG. 1996. The effects of disequilibria in the uranium and thorium decay chains on burial dose rates in fluvial sediments. *Quat. Sci. Rev. (Quat. Geochronol.)* 15:751–60

Olley JM, Pietsch T, Roberts RG. 2004b. Optical dating of Holocene sediments from a variety of geomorphic settings using single grains of quartz. *Geomorphology* 60:337–58

Owen LA, Bailey RM, Rhodes EJ, Mitchell WA, Coxon P. 1997. Style and timing of glaciation in the Lahul Himalaya, northern India: a framework for reconstructing late Quaternary palaeoclimatic change in the western Himalayas. *J. Quat. Sci.* 12:83–109

Perkins NK, Rhodes EJ. 1994. Optical dating of fluvial sediments from Tattershall, U.K. *Quat. Sci. Rev.* 13:517–20

Pietsch TJ, Olley JM, Nanson GC. 2008. Fluvial transport as a natural luminescence sensitiser of quartz. *Quat. Geochronol.* 3:365–76

Porat N, Duller GAT, Roberts HM, Wintle AG. 2009. A simplified SAR protocol for TT-OSL. *Radiat. Meas.* 44:538–42

Prescott JR, Hutton JT. 1994. Cosmic ray contributions to dose rates for luminescence and ESR dating: large depths and long-term time variations. *Radiat. Meas.* 23:497–500

Prescott JR, Stephan LG. 1982. The contribution of cosmic radiation to the environmental dose for thermoluminescent dating. Latitude, altitude and depth dependences. *PACT J. (Council of Europe)* 6:17–25

Preusser F, Chithambo ML, Götte T, Martini M, Ramseyer K, et al. 2009. Quartz as a natural luminescence dosimeter. *Earth-Sci. Rev.* 97:184–214

Rhodes EJ. 1988. Methodological considerations in the optical dating of quartz. *Quat. Sci. Rev.* 7:395–400

Stands as a key paper for the development of SAR OSL.

Represents another key paper for the development of SAR OSL.

Provides a thorough, lengthy review of quartz OSL.

Rhodes EJ. 2000. Observations of thermal transfer OSL signals in glacigenic quartz. *Radiat. Meas.* 32:595–602

Rhodes EJ. 2007. Quartz single grain OSL sensitivity distributions: implications for multiple grain single aliquot dating. *Geochronometria* 26:19–29

Rhodes EJ, Bailey RM. 1997. The effect of thermal transfer on the zeroing of the luminescence of quartz from recent glaciofluvial sediments. *Quat. Sci. Rev. (Quat. Geochronol.)* 16:291–98

Rhodes EJ, Bronk-Ramsey C, Outram Z, Batt C, Willis L, et al. 2003. Bayesian methods applied to the interpretation of multiple OSL dates: high precision sediment age estimates from Old Scatness Broch excavations, Shetland Isles. *Quat. Sci. Rev.* 22:1231–44

Rhodes EJ, Fanning PC, Holdaway SJ. 2010. Developments in optically stimulated luminescence age control for geoarchaeological sediments and hearths in western New South Wales, Australia. *Quat. Geochronol.* 5:348–52

Rhodes EJ, Pownall L. 1994. Zeroing of the OSL signal in quartz from young glaciofluvial sediments. *Radiat. Meas.* 23:329–33

Rhodes EJ, Singarayer JS, Raynal J-P, Westaway KE, Sbihi-Alaoui FZ. 2006. New age estimates for the Palaeolithic assemblages and Pleistocene succession of Casablanca, Morocco. *Quat. Sci. Rev.* 25:2569–85

Richards BWM, Benn DI, Owen LA, Rhodes EJ, Spencer JQ. 2000. Timing of Late Quaternary glaciations south of Mount Everest in the Khumbu Himal Nepal. *Geol. Soc. Am. Bull.* 112:1621–32

Rittenour TM. 2008. Luminescence dating of fluvial deposits: applications to geomorphic, palaeoseismic and archaeological research. *Boreas* 37:613–35

Rodnight H, Duller GAT, Wintle AG, Tooth S. 2006 Assessing the reproducibility and accuracy of optical dating of fluvial deposits. *Quat. Geochronol.* 1:109–20

Sanderson DCW, Murphy S. 2010. Using simple portable OSL measurements and laboratory characterisation to help understand complex and heterogeneous sediment sequences for luminescence dating. *Quat. Geochronol.* 5:299–305

Singarayer JS, Bailey RM. 2003. Further investigations of the quartz optically stimulated luminescence components using linear modulation. *Radiat. Meas.* 37:451–58

Singarayer JS, Bailey RM, Rhodes EJ. 2000. Potential of the slow component of quartz OSL for age determination of sedimentary samples. *Radiat. Meas.* 32:873–80

Singarayer JS, Bailey RM, Ward S, Stokes S. 2005. Assessing the completeness of optical resetting of quartz OSL in the natural environment. *Radiat. Meas.* 40:13–25

Smith BW, Aitken MJ, Rhodes EJ, Robinson PD, Geldard DM. 1986. Optical dating: methodological aspects. *Radiat. Prot. Dosim.* 17:229–33

Smith BW, Rhodes EJ. 1994. Charge movements in quartz and their relevance to optical dating. *Radiat. Meas.* 23:581–85

Smith BW, Rhodes EJ, Stokes S, Spooner NA, Aitken MJ. 1990. Optical dating of sediments: initial results from Oxford. *Archaeometry* 32:19–31

Spencer JQ, Owen LA. 2004. Optically stimulated luminescence dating of Late Quaternary glaciogenic sediments in the upper Hunza valley: validating the timing of glaciation and assessing dating methods. *Quat. Sci. Rev.* 23:175–91

Stevens T, Thomas DSG, Armitage SJ, Lunn HR, Lu H. 2007. Reinterpreting climate proxy records from late Quaternary Chinese loess: a detailed OSL investigation. *Earth-Sci. Rev.* 80:111–36

Stone AEC, Thomas DSG. 2008. Linear dune accumulation chronologies from the southwest Kalahari, Namibia: challenges of reconstructing late Quaternary palaeoenvironments from aeolian landforms. *Quat. Sci. Rev.* 27:1667–81

Wallinga J, Hobo N, Cunningham AC, Versendaal AJ, Makaske B, et al. 2010. Sedimentation rates on embanked floodplains determined through quartz optical dating. *Quat. Geochronol.* 5:170–75

Wang XL, Wintle AG, Lu YC. 2007. Testing a single-aliquot protocol for recuperated OSL dating. *Radiat. Meas.* 42:380–91

Weil JA. 1984. A review of electron spin spectroscopy and its application to the study of paramagnetic defects in crystalline quartz. *Phys. Chem. Miner.* 10:149–65

Provides an excellent survey particularly for fluvial and neotectonic OSL applications.

Westaway KE. 2009. The red, white and blue of quartz luminescence: a comparison of D_e values derived for sediments from Australia and Indonesia using thermoluminescence and optically stimulated luminescence. *Radiat. Meas.* 44:462–66

Wintle AG. 1973. Anomalous fading of thermoluminescence in mineral samples. *Nature* 245:143–44

Wintle AG, Murray AS. 1999. Luminescence sensitivity changes in quartz. *Radiat. Meas.* 30:107–18

Wintle AG, Murray AS. 2006. A review of quartz optically stimulated luminescence characteristics and their relevance in single-aliquot regeneration dating protocols. *Radiat. Meas.* 41:369–91

Contents

Indexes

Errata

An online log of corrections to *Annual Review of Earth and Planetary Sciences* articles
may be found at http://earth.annualreviews.org

ANNUAL REVIEWS

It's about time. Your time. It's time well spent.

New From Annual Reviews:

Annual Review of Statistics and Its Application

Volume 1 • Online January 2014 • http://statistics.annualreviews.org

Editor: **Stephen E. Fienberg,** *Carnegie Mellon University*

Associate Editors: **Nancy Reid,** *University of Toronto*

Stephen M. Stigler, *University of Chicago*

The *Annual Review of Statistics and Its Application* aims to inform statisticians and quantitative methodologists, as well as all scientists and users of statistics about major methodological advances and the computational tools that allow for their implementation. It will include developments in the field of statistics, including theoretical statistical underpinnings of new methodology, as well as developments in specific application domains such as biostatistics and bioinformatics, economics, machine learning, psychology, sociology, and aspects of the physical sciences.

Complimentary online access to the first volume will be available until January 2015.

Access this and all other Annual Reviews journals via your institution at **www.annualreviews.org**.

ANNUAL REVIEWS | Connect With Our Experts

Tel: 800.523.8635 (us/can) | Tel: 650.493.4400 | Fax: 650.424.0910 | Email: service@annualreviews.org